PHYSICAL REVIEW B
CONDENSED MATTER

THIRD SERIES, VOLUME 48, NUMBER 6 1 AUGUST 1993-II

High-pressure liquid-liquid phase change in carbon

M. van Thiel and F. H. Ree
Lawrence Livermore National Laboratory, University of California, Livermore, California 94550

(Received 20 April 1992; revised manuscript received 16 December 1992)

The likelihood of a first-order liquid-liquid phase change in carbon from a mostly graphitic configuration to one that is more tetrahedral in character is explored. Liquid-phase changes in other materials are noted. Pertinent data on liquid carbon are reviewed and the model is briefly described. The model is consistent with a positive diamond-melting-line slope. Constraints on the strain energy between graphitic and diamondlike liquid clusters allow a phase diagram with a liquid-liquid transition and a graphite-liquid-liquid triple point. An upper limit on the strain energy is the constraint that the graphite melting line should have a reasonable curvature that agrees with melting-line data. The transformation of liquid structure from graphitic to diamondlike under compression significantly increases the compressibility.

I. INTRODUCTION

In previous work[1] a three-phase carbon-equation-of-state (EOS) theory was developed to simulate the high-pressure and temperature properties of carbon formed in high-energy processes. We assumed there that the liquid should consist of a single phase whose properties change smoothly with pressure. Our recent examination of this model, as well as work performed elsewhere[2-8] on other materials, indicates that this may be an incorrect assumption. This paper presents results obtained by removing this assumption.

Phase changes in the liquid state are not uncommon. Recent pair-distribution and structure-factor data[2] show definite pressure-dependent changes in the near-neighbor distances of Bi, Ga, and Se with rather startling changes for Bi between 4.7 and 7.3 GPa. Popova[3] has determined the existence of three liquid phases in Bi. The slope of the resistance vs temperature curve of Te indicates a change from semiconducting to metallic character[4] between 0.9 and 0.5 GPa, while Se has an apparently first-order insulator-metal[5] transition across a line defined by the two (P,T) points (3.7 GPa, 900 K) and (1.5 GPa, 1250 K) with an apparent critical point near the higher (P,T) point. In liquid iodine Brazhkin *et al.*[6] found a band closure and a metal-metal transition with a $dP/dT \approx 0$, indicating a large volume change. Sulfur has at least three liquid phases:[7,8] two insulating phases and a metallic phase.

The above observations suggest that liquid graphite could also exhibit a multiphase liquid structure. We review pertinent work on graphite and present a model that exhibits graphitic and diamondlike liquid phases.

II. EXPERIMENTAL EVIDENCE

The suggestion that liquid carbon may have several phases and may transform to a metallic liquid above 0.1 GPa was made[9] more than 10 years ago, but has so far not been substantiated with quantitative calculations. A great deal of work has been done on graphite, and some good review articles are available.[10-12] Much still needs to be learned about the relationship between the thermodynamic properties of liquid carbon and its structure, although some structural information is becoming available from first-principles molecular-dynamics calculations.[13] In particular, strain energy is reduced if atoms with similar electronic structure form clusters and this study shows evidence of the existence of clusters of tetrahedral, planar (ring), and linear structures in a low-pressure liquid. While such clustering is of special interest in the study of amorphous carbons, it is also of interest in a liquid near the melting transition at low pressure[13] (0.01–8 GPa) and at high pressure,[14] since they suggest that structural transitions are also likely in the liquid. In the 100-GPa pressure range, large ring and chain structures disappear, as expected from the denser packing of the atoms.

At high temperatures the interatomic distances and angular relationships become random and first-order transitions less likely. The quantitative connection of the electronic configuration to a macroscopic model as presented

0163-1829/93/48(6)/3591(9)/$06.00

here can be made only with an accurate definition of statistical averages at those temperatures at which the distribution of possible structures is not too diffuse. Since this must be done with first-principles calculations that track the electronic degrees of freedom, it is still a very time-consuming problem with today's computers.

A reasonable liquid electronic density of states[13] has, however, been derived from such calculations. The computed resistivity of 140 $\mu\Omega$ cm is somewhat larger than the a-axis resistivity (ρ_a) of the most highly ordered graphite crystals or pyrolytic structures (40–60 $\mu\Omega$ cm),[15] but lower than less ordered structures (up to $\rho_a = 500\ \mu\Omega$ cm), or amorphous solids with values as high as 1000 $\mu\Omega$ cm, comparable to the resistivity across the graphite planes of ordered crystals. Although the electronic degrees of freedom have a minor effect on the P, ρ, T properties computed with our model, they are an important link to liquid structure. We therefore summarize the principal experimental results.

The aforementioned low liquid resistivity is consistent with the experimentally observed decrease in resistivity on melting. At pressures between 1 and 10 GPa, the work of Bundy[16] shows a definite resistivity decrease on melting of 20%–50%. In addition, his electrical pulse melting of graphite indicates some notable differences between the pressure-independent resistivity ρ_{s0} ($\approx 400\ \mu\Omega$ cm) of his annealed, cold, spectroscopic graphite and its liquid phase. Bundy[16] heated spectroscopically pure polycrystalline graphite into the melt in about 5 ms. The liquid resistivity decreases with pressure. At pressures between 5 and 10 GPa, he observed liquid resistivities $[\rho_L(P)]$ down to 30% below ρ_{s0}. Between 1 and 5 GPa, $\rho_L(P)$ appears to be somewhat higher than ρ_{s0} and is as large as $2\rho_{s0}$ at 0.9 GPa. The slope $(\partial\rho_s/\partial T)_P$ of the solid decreased with pressure, suggesting a more semiconducting character at higher pressures. However, a possible discontinuous change in the resistivity of the liquid, and, therefore, a phase change, is not obvious from the data.

A similar trend is implied by the increase in reflectivity of pyrolytic graphite when it is pulse heated well into the liquid phase with a femtosecond laser pulse.[17] These experiments show that the resistivity drops on melting and decreases with increasing pressure.

Below 0.4 GPa neither the polycrystalline carbon of Gathers, Shaner, and Young[18] nor the graphite of Baitin *et al.*[19] showed any significant changes in resistivity when they melt. Their samples were heated with current pulses (respectively, ~20 and ~2000 μs long) in an argon pressure medium, at pressures between 0.1 and 0.4 GPa. The resistance of the sample increases smoothly through the melting point. The resistivity of the melting polycrystalline carbon[18] is about 1000 $\mu\Omega$ cm and increases as the melt gets hotter, as might be expected under constant-pressure heating of a metallic liquid. The resistivity of the graphite of Baitin *et al.*[19] was not listed, but may be inferred from their sample description to be about 100 $\mu\Omega$ cm in the melt and also increasing with temperature.

Two types of measurements initially appeared to yield contradictory results for the resistivity change on melting. Namely, Steinbeck and co-workers[20] reported that a current pulse (20-A maximum) of 28-μs duration reduced the a-axis resistance of carbon whiskers, annealed to 2000 and 3100 K at ambient pressure, by about a factor of 4–5 at the melting point. By contrast, Malvezzi, Bloembergen, and Huang[21] showed that a 20-ps-long, $\lambda = 0.53\ \mu$m laser pulse produced a reduction in reflectivity in a pyrolytic graphite surface of up to 30% for as long as 600 ps, whereupon the surface presumably resolidified and/or vaporized. This would suggest a decrease in the number of free electrons on melting. However, more recent work by Seibert *et al.*[22] showed that the reduction in reflectivity was due to expanded material. Femtosecond resolution is required to see an increase of reflectivity[17] of the undisturbed but heated material between 1 and 4 ps after the heating pulse. Resistivities computed from this work[17] (350–600 $\mu\Omega$ cm) are in the same range as those measured by Bundy.[16] The samples in this work reached significant temperatures, which would ordinarily increase the liquid resistivity. Instead, the temperature increased the reflectivity and, therefore, the conductivity. Calculated temperatures range from 5000 to 100 000 K depending on the fluence of their heating pulse. But pressure is also a factor to consider in making comparisons with other data. On this experimental time scale, the heating occurs essentially at constant density. At a density of 2.26 g/cm^3 and 5000 K, $P \cong 5$ GPa, and at 6000 K, $P \cong 8.5$ GPa as determined by the model we present below. Here too, therefore, pressure seems to enhance the metallic character of the liquid as does melting increase the metallic character of graphite. In any case, the pulse heating of a graphite whisker and the femtosecond laser heating agree on the decrease of resistivity on melting.

The carbon whiskers mentioned above yielded a resistivity of about 70 $\mu\Omega$ cm after annealing[23] to 3100 K. The resistivities of Heremans and co-workers and of Steinbeck and co-workers[20] were, therefore, lower than those of Bundy[16] and Baitin *et al.*[19] and considerably lower than those of the amorphous samples of Gathers, Shaner, and Young,[18] in spite of the imperfections in the crystal structure of the whisker. However, the large variability of whisker sizes complicates the determination of the resistivity. Furthermore, the low resistivity of whiskers may be due to contamination by the heavy metal used in growing them. The difference in observed resistivities between Refs. 17 and 20 may, therefore, not be significant. The absence of a resistivity change on melting (of carbon samples pressurized by an atmosphere of compressed argon) observed by Baitin *et al.* and Gathers, Shaner, and Young remains an important anomaly yet to be resolved. But sample contamination by nonconducting species may explain the absence of a resistivity change on melting.

More significant is the decrease of the liquid resistivity with pressure observed by Bundy[16] and by Reitze, Ahn, and Downer.[17] While neither source shows a sharp discontinuity in liquid properties that would signal a first-order phase transition, such a possibility cannot be excluded. Feraz and March[9] do interpret Bundy's experiments as an indication of a liquid-liquid transition. The phase change proposed in this work lies within the pressure range where Bundy observed a change from $\rho_L(P)<\rho_{s0}$ to $\rho_L(P)>\rho_{s0}$. Below, we present additional evidence that such a phase change may exist in liquid carbon.

III. THEORY

We have used a macroscopic multiphase model of carbon to compute the EOS of liquid carbon and its phase diagram. The algorithm is sufficiently simple and fast to serve as a data source for more complex calculations that require a carbon EOS.

In our model two liquid phases are produced based on a scaling formalism, which, applied to the graphite phase, produces a "graphitic" liquid and, applied to the diamond solid phase, produces a "diamondlike" liquid. A possible carbonic liquid has not been considered, since the properties of the proposed solid phase[24] are not known. The concept of two materials mixing is here extended to the mixing of the two liquid types. The liquid consists of "diamondlike" liquid clusters and "graphitic" liquid clusters. The atomic configuration of these clusters is not defined by this model, although one expects that the graphitic liquid will have more open structures than the more three-dimensional diamondlike liquid with its essentially tetrahedral network. Changes in volume across the phase lines can, in principle, offer some qualitative connection to microscopic structures when the volume of such structures is quantified. The phase separation in the mixed liquid is due to a strain energy in the theory that mixes the graphitic and diamondlike liquids.

A. Solid carbon

The major features of this model have been discussed earlier,[1,25] but will be highlighted here with the indicated changes. The adiabatic approximation is assumed in the description of the energy (E_s) and pressure (P_s) of the solid:

$$\begin{aligned} E_s(V,T)&=E_K(V)+E_{\mathrm{th},l}(V,T)+E_{\mathrm{th},e}(T)\ ,\\ P_s(V,T)&=P_K(V)+P_{\mathrm{th},l}(V,T)+P_{\mathrm{th},e}(V,T)\ . \end{aligned} \tag{1}$$

The three terms to the right of the equal sign are a 0-K term (subscript K) and thermal contributions from lattice (subscript *l*) and electronic (subscript *e*) degrees of freedom.

We use the Birch equation to describe $P_K(V)$,

$$\begin{aligned} P_K(V)&=\tfrac{3}{2}B_{0\,\mathrm{K}}\{-B_k'\eta^3+(1+2B_k')\eta^{7/3}\\ &\quad-(1+B_k')\eta^{5/3}\}f(\eta)\ ,\\ f_P(\eta)&=1 \quad \text{for } \eta>1 \end{aligned} \tag{2}$$

and

$$f_P(\eta)=(\eta^2+\eta^{-2})/2 \quad \text{for } \eta<1\ ,$$

where the function $f_P(\eta)$ excludes high (and unphysical) pressures at large volume expansions in the equation for graphite (for diamond $f_P\equiv1$). Here $B_{0\,\mathrm{K}}$ is the bulk modulus at $P=0$ and $T=0$, $B_k'=0.75(4-B_0')$, B_0' being the pressure derivative of the bulk modulus at 0 K, and $\eta=V_{0\,\mathrm{K}}/V$. This equation is then integrated to yield $E_K(V)$ as a function of V.

Thermal energies are determined by integrating the heat capacity

$$C_{VS}=C_{Vl}+g_eT\ , \tag{3}$$

where C_{Vl} is the Einstein heat capacity of the lattice and g_eT is the electronic component. Thermal pressures for the lattice and electrons are represented by a Grüneisen description ($P_{\mathrm{th}}=\gamma E_{\mathrm{th}}$) with appropriate γ's $[\gamma=-V(\partial V/\partial E)_V]$ for the electronic (γ_e) and lattice (γ_l) terms:

$$\gamma_e(V)=(V/V_0)\gamma_{0,e}(V)\ , \tag{4}$$

$$\begin{aligned} \gamma_l(V)&=(V/V_0)\gamma_{0,l}(V)\\ &=(V/V_0)\gamma_{00,l}\{1+\delta_\gamma[1+\tanh(z)]\}\ , \end{aligned} \tag{5}$$

where $z(=(V_\gamma-V)/\delta V_\gamma)$ allows for the increase of the graphite $\gamma_{0,l}(\gamma_{00,l}=0.35)$ when the in-plane and out-of-plane vibron amplitudes become comparable at high pressures. The constants V_γ ($=2.64$ cm^3/mol) and δV_γ ($=0.78$ cm^3/mol) define the density range for this change in the graphite EOS with an amplitude of $\delta_\gamma=3$. For the cubic diamond lattice with a more normal $\gamma_{00,l}$ of 1.15, δ_γ is set to 0.

The electronic γ for graphite and the corresponding liquid (see below) is set to the free-electron value ($\gamma_{e,0}=0.24$). Solid diamond is described as an insulator even though a certain amount of hexagonal diamond is formed in shock-compression experiments. The latter has a Fermi energy that decreases with pressure,[26] which will have a small effect on the thermal energy under shock compression at megabar pressures.

Since this is a high-temperature model, we may use Einstein functions for the nuclear thermal energy $E_{\mathrm{th},l}=E_E(V,T)$ in Eq. (1) and the solid-lattice heat capacity $C_{V1}=C_E(V,T)$ in Eq. (3). The volume dependence is introduced through the Einstein temperature $\Theta(V)$ by

$$\frac{d\ln\Theta(V)}{d\ln V}=\gamma_i(V)=\frac{\gamma_{0,i}(V)}{V_0}V\ . \tag{6}$$

The electronic heat capacity $C_{V,e}=g_eT$ and energy $E_{\mathrm{th},e}=0.5g_eT^2$ are independent of volume. The low-T value of g_e was chosen for graphite, while g_e for diamond is set to 0. The low-temperature Einstein heat capacity is known to be only approximate. The thermal energy and entropy are, therefore, corrected with a constant term to yield the experimental heat of formation and entropy at 298 K.

The equations of state for graphite and diamond are well known from shock-wave data[25,27] and theoretical calculations on diamond,[28] and are accurately represented by Eqs. (1)–(6).[25]

B. Liquid carbon

The electronic degrees of freedom of graphitic liquid are described by the same g_e and γ_e as were used for the solid phase. In view of the low-pressure results described in a previous section, we assigned the increase in conductivity to the diamondlike liquid. For liquid diamond we have used the result from the INFERNO (Ref. 29) atom-in-a-cell model to determine g_e ($=6.038\ 10^{-5}$ R) and γ_{e0} ($=1.1$).[1]

For the nuclear degrees of freedom, we adopt Grover's model,[30] which is based on melting calculations of hard-sphere[31] and soft-sphere systems.[32] In addition, experimental heat capacities are available for a number of low melting metals over a sufficient temperature range in the liquid region to show that the trends are similar. It was noted that the heat capacity of the liquid can be scaled to the melting temperature T_m with a reduced temperature $\tau = T/T_m$ by the function,[30]

$$C_{VL} = C_{Vl} + g_{e,L}T - 1.5R\frac{\alpha\tau}{1+\alpha\tau} , \qquad (7)$$

where the subscript L refers to the liquid phase, R is the gas constant, and $C_{V,l}$ is the aforementioned Einstein heat capacity of the solid. While Eq. (7) has the proper limits near melting and at high temperatures, the details of the behavior near the melting point are not accurately represented. The observed curvature in the temperature dependence of the solid and liquid heat capacities near the melting point can, however, be attributed to pre- and postmelting phenomena such as defect formation. Grover noted that if the deviation from the above model is calculated and added to the experimental entropy of melting (ΔS_m), the hard-sphere entropy change is obtained for a number of metals[33] (Na,K,Pb,In,Hg) within 10%.

The suggestion that the hard-sphere model should be a prototype for melting phenomena is further supported by applicability of the Lindemann law[34] to the change of melting temperature (T_m) with pressure. In particular, the observed linear behavior of T_m with pressure is predicted by the Lindemann law and the rapid decrease of the Grüneisen γ with pressure.[30,35] Since this melting model is based essentially on repulsive forces, its usefulness suggests that the interatomic forces of graphite and diamond at and above melting are controlled primarily by the repulsive part of the nearest-neighbor potentials.

Deviations do, of course, exist. Insulators, metals, and semiconductors such as Ar, Al, Bi, Sn, Ga, C, and Si have relatively high entropies of melting, ΔS_m, between $1.8R$ and $3.5R$ as opposed to the hard-sphere entropy change of $1.15R$. But in the case of argon ($\Delta S_m = 1.8R$), compression rapidly reduces ΔS_m to approximately the hard-sphere value.[36] Therefore, while the attractive part of the potential still plays some role, pressure tends to eliminate it. On the strength of the above argument, the Grover model for graphite and diamond is the best available model for our purpose.

Given ΔS_m, the liquid energy is obtained by integrating Eq. (7) to yield[30]

$$E_L(V,T) = E_l(V,T) + E_{\mathrm{th},e}(T) + RT_m\left\{\frac{\Delta S_m}{R} - \frac{3}{4}\alpha + \frac{3}{2}\tau\left[\frac{\ln(1+\alpha\tau)}{\alpha\tau} - 1\right]\right\}, \qquad (8a)$$

where

$$E_l(V,T) = E_K(V) + E_{\mathrm{th},l}(V,T) \qquad (8b)$$

and $E_{\mathrm{th},l}$ is specific for the liquid. The third term on the right-hand side of Eq. (8a) is a correction term due to the entropy of melting and the liquid correction to the heat capacity shown in Eq. (7). For graphite we have adopted a value close to that measured by Bundy[16] ($\Delta S_m/R = 2.7$), while for diamond we use the hard-sphere value ($\Delta S_m/R = 1.15$). Given the entropy of melting, the liquid heat capacity [Eq. (7)] may also be integrated to give the entropy and, therefore, the Helmholtz ($F = E - TS$) and the Gibbs ($G = F + PV$) free energies of liquid graphite and diamond:

$$G_L(P,T) - F_l(P,T) = RT_m\left\{(1-\tau)\frac{\Delta S_m}{R} - \frac{3}{4}\alpha + \frac{3}{2}\tau\left[\frac{1+\alpha\tau}{\alpha\tau}\ln(1+\alpha\tau) - 1\right]\right\} + F_{\mathrm{th},e}(T) + PV . \qquad (9)$$

The pressure of the liquids, P_L, is given by

$$P_L = P_l + \gamma_{eL}E_{\mathrm{th},e} + \lambda(E_L - E_l - E_{\mathrm{th},e})/V , \qquad (10)$$

$$\lambda = -\frac{d\ln T_m}{d\ln V} . \qquad (11)$$

This melting-line slope is defined by the Linemann law[34] discussed below.

C. Lindemann law

The Lindemann criterion states that the root-mean-square vibrational amplitude (δ) for cubic systems with lattice parameter a at the melting point is

$$\frac{\langle\delta\rangle}{a} = \mathrm{const} . \qquad (12)$$

This yields the usual form of the Lindemann law,[37]

$$T_m = \mathrm{const} \times \Theta^2 M V^{2/3} . \qquad (13)$$

From Eqs. (6) and (11), we now get the simple form $\lambda = 2\gamma - \frac{2}{3}$, with γ defined in Eq. (5).

This form is not applicable to highly anisotropic systems.[38] Hence if it is applied to graphite (with a $\gamma \cong \frac{2}{3}$), it yields the wrong melting-line slope. The possibility that γ is too small at the melting point can be excluded. The expansion coefficient[39] is known to $T = 3000$ K and is well represented by the compressibility and γ. If Eq. (6) is modified to allow $\gamma(V)$ to increase sufficiently between 3000 and 4500 K to yield the proper melting-line slope, Eq. (2) predicts a negative $(\partial P/\partial\rho)_T$ at high temperatures, at densities defined by z in Eq. (5).

The proper Lindemann criterion depends on the particular lattice type it is applied to. If the ratios of the lattice constants are not constant with compression, one cannot relate the vibrational amplitude of the mode that is active in the melting process to a single lattice parameter. The graphitic system is an extreme case. For a graphitic system, the criterion can be rewritten as

$$\frac{\langle d \rangle}{(1-f)a+fc}=\text{const} \tag{14}$$

to allow for a weak effect of changes in the c-axis dimension. The value of $f=0.01\rho^{1/2}$ (with ρ in g/cm^3) is determined by the low-pressure slope of the melting line, the approximate symmetry of the (P,T_m) curve around $P=5$ GPa, offers a maximum for the difference $(T_{m,\max}-T_{tP})$ between the maximum in the graphite melting point and the lower triple point, and affords the best melting-line fit. It is further constrained by the known density dependence of the c/a ratio[39,40] $(=0.25+2.53/\rho$, with ρ in g/cm$^3)$. Following the derivation as for cubic systems,[34] the melting temperature for the laminar structure of graphite is

$$T_m=\text{const}\times\Theta^2MV^{2/3}(a/c)^{2/3}[(1-f)+f(c/a)]^2 \ . \tag{15}$$

This is the form used for graphite. For diamond the standard form [Eq. (13)] is used.

D. Mixed liquid

Equations (7)–(15) define the "scaled" liquid phases for graphite or diamond based on the solid-phase equations of state defined by Eqs. (1)–(6).

Far from the graphite-diamond-liquid triple point, the diamond-liquid transition may be defined by the Gibbs free energies of the solid and its scaled liquid EOS and similarly for graphite. But near the triple point, the two types of liquid must be allowed to mix. Otherwise, the model would predict a quadruple point that includes a liquid-liquid transition (instead of a triple point), a situation excluded by the Gibbs phase rule. To satisfy this constraint, we use the theory of mixtures[41] and minimize G_{liq} with respect to the atom fraction x of liquid diamond to obtain

$$\begin{aligned}G_{\text{liq}}={}&xG_{Ld}+(1-x)G_{Lg}\\&+RT[x\ln x+(1-x)\ln(1-x)]+A_s(T,P,x) \ ,\end{aligned} \tag{16a}$$

where we use

$$A_s(T,P,x)=RT\left[\frac{A_{S,0}}{1+(P/P_0)^{3/2}}\right]x(1-x) \ . \tag{16b}$$

This allows the mixing of the two types of liquid. G_{Ld} and G_{Lg} are defined by Eq. (9) for diamondlike and graphitelike liquids. The distribution of the two liquid structures is random[41] with fractions x and $1-x$, respectively, resulting in the ideal logarithmic entropy of mixing terms in Eq. (16). The random mixture of graphitic and diamondlike structures can be either atoms or clusters of equal size (n). Then we can unambiguously define

$$x=\frac{N_d/n}{N_d/n+N_g/n}=\frac{N_d}{N_d+N_g} \ , \tag{17}$$

independent of n, with N being the total number of atoms in the mixture. The strain energy (A_s) does of course depend on n. Since the strain energy is a surface effect $(nA_s\sim n^{2/3})$, the temperature dependence of A_s $(\sim 1/n^{1/3})$ in Eq. (16b) implies that $n^{1/3}\sim 1/T$, which was arbitrarily chosen for computational convenience. But the pressure dependence is consistent with the barrier to transformation computed by Fahy, Louie, and Cohen,[40] in so far as the quantity in square brackets [Eq. (16b)] is small at their spontaneous transformation pressure near 80 GPa. The magnitude of A_s affects the compressibility of the liquid near 6 GPa where the value of x, and the diamondlike character of the liquid, rapidly increases. Sufficiently large values of A_s cause the liquid to separate into two phases.

IV. LIQUID STRAIN ENERGY

The boundaries between graphitic and diamondlike liquid clusters (and for sufficiently small clusters the clusters themselves) are energetically of the order of a transition state as defined in Arhenius kinetics.[42] Experimental data of diamond-to-graphite transformation rates near the melting line are the best source for this transition energy. Diamond with a vibrational shear mode frequency $\nu=3.8\times10^{13}$ s^{-1} would have a transformation probability

$$\mathcal{P}=0.5\nu\exp(-\varepsilon^*/kT) \ , \tag{18a}$$

if a single atom could define the activated state. Here the exponential term gives the fraction of atoms[43] in the activated state and ν the frequency with which the transition configuration is approached. But a single atom transforming from a diamond to a graphitic configuration does not form a stable nucleus. If a stable nucleus consists of n atoms vibrating in phase to and over the transition barrier, the probability may be written

$$\mathcal{P}^*=0.5\nu^*\exp(-n\varepsilon^*/kT) \ . \tag{18b}$$

The rate has been determined experimentally[44] near the melting line of graphite. A hot graphite rod insulated with diamond powder initiates a transformation of the diamond to graphite at about $T=3800-4200$ K in the graphite stable region of the phase diagram and over a time interval of about 1 ms. Using that as the e-fold time [for $dN/N(t)=\mathcal{P}^*dt$] and using $\nu^*\approx\wp^{n-1}\nu$, where $\wp$ is the probability that a neighboring atom has the proper phase relationship, we may compute $\varepsilon^*=\varepsilon^*(n)$ from

$$-n\varepsilon^*\approx kT\left[\ln\frac{2}{e\Delta t\nu^*}\right]=3.7\text{ eV} \tag{19}$$

and get the results in Fig. 1 for two reasonable values of $\wp$ and the probable extremes of the uncertainty range of the experimental temperature. The range of possible cluster sizes is between 2 and 12 or 16 atoms for the two vibrational phase constraints chosen and with the given transformation temperature.

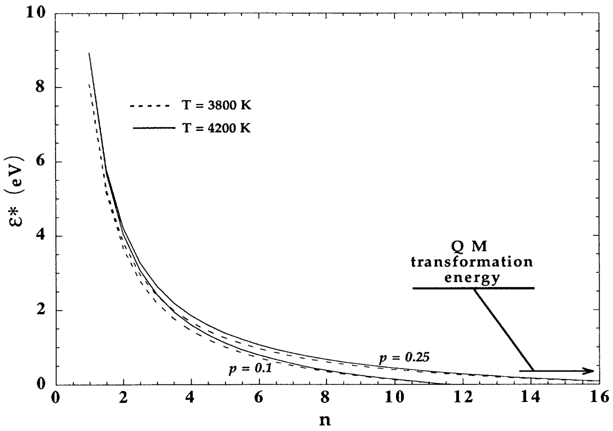

FIG. 1. Arhenius activation energy per atom for a carbon cluster of *n* particles that, at the given temperatures, gives the 1-ms transformation time indicated by Bundy (Ref. 44). The quantum-mechanical lattice transformation energy of Fahy, Louie, and Cohen (Ref. 40) is indicated by a labeled arrow.

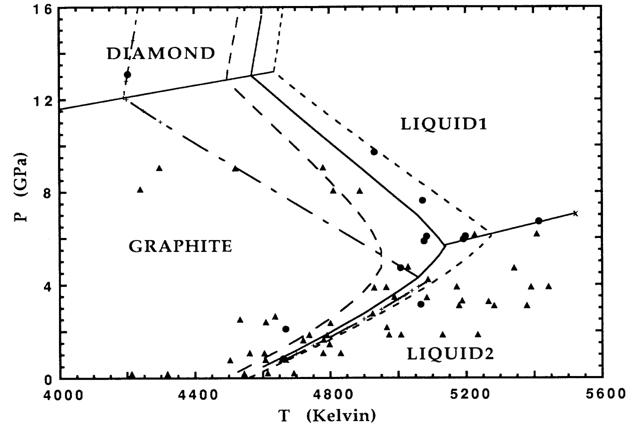

FIG. 2. Phase diagram of carbon in the graphite stable pressure range. The measurements of Fateeva and Vereshchagin (Ref. 47) ▲ and Bundy's measurements (Ref. 16) (●). Melting and liquid-liquid transitions this theory: $A_{s,0}=2.0$ (long-dashed line), $A_{s,0}=2.4$ (solid line), $A_{s,0}=2.8$ (short-dashed line), and $A_{s,0}=2.8$, with T_{m0} (diamond) reduced by 12% (short and long dashes). A possible liquid-liquid critical point (×) is also shown.

A minimum strain energy per atom may be estimated from *a priori* quantum-mechanical calculations of the crystal along its minimum-energy transformation path. Local-density theory[40] predicts a maximum along that path of 0.67 eV per two-atom unit cell. Similar although somewhat higher values are calculated for diamond-BC8 transformations with a pseudopotential method.[45] This is the energy for two atoms transforming simultaneously with the rest of the lattice and neglects the strain energy at the boundary of a nucleus of transformed material. We therefore may take 0.33 eV/atom as the minimum energy of the activated state. Referring to Fig. 1, we note that the largest possible clusters consist of 8–11 atoms.

More detailed graphite-to-diamond transformation measurements than the diamond-to-graphite transformation of Ref. 44 have been made[46] over 5-min time intervals at 2500–3500 K in the diamond stable region and at 9 GPa. The analysis yields a nucleus size of about 16 atoms and $n\varepsilon=1.0$ eV. At these lower temperatures and longer transformation times, the mechanisms may be quite different. This exercise, therefore, offers a fairly broad range of values for $A_{s,0}$ in Eq. (16). By this analysis, the value of $A_{s,0}$ may therefore be small for large clusters and approaches the sublimation energy for one- or two-atom clusters. Considerations of the structure of the phase diagram offers a closer estimate of the liquid cluster size.

V. DISCUSSION

Minimizing G_{liq} in Eq. (16) with respect to x and determining the condition $G_{\text{liq}}(T,P)=G_{s,i}(T,P)$ (where i is d for diamond or g for graphite) gives the melting lines in the phase diagram in Fig. 2. The graphite-to-diamond transition is similarly determined by the condition $G_{s,d}(T,P)=G_{s,g}(T,P)$. A significant quantity that constrains $A_{s,0}$ is the large difference between the minimum and maximum experimental T_m values of the graphite-liquid phase boundary. The curvature of a graphite-liquid boundary has been determined experimentally by Bundy's electrical[16] measurements and the optical[47] measurements of Fateeva and Vereshchagin. The low-pressure slope given by the model is determined by f in Eq. (14) and γ_l in Eq. (5). The latter controls the slope of Θ [Eq. (6)]. Both control the slope of the melting line through the liquid-graphite component. Equation (16) shows that the largest contribution of A_s to G occurs near $x=\frac{1}{2}$. As $A_{s,0}$ is increased, the difference between small values of x below and large values above 5 GPa becomes larger, as does the difference between the lower and upper limits of the melting temperature.

The data of Fateeva and Vereshchagin and Bundy's interpretation of their data indicate a gas-liquid-graphite triple-point temperature of 4000 K, the best data available at the time that the high-pressure melting line was measured.[48] The more recent measurements of the graphite-liquid-vapor triple point place its temperature between 4500, according to Cezairliyan and Miller,[49] and 5000 K, according to Baitin *et al.*[19] The higher triple-point temperatures imply the need for a correction to the melting lines, but they do not change the shape of the curves. The experimental data was corrected to the 4500 K triple point by adding the same ΔT to all points.

But aside from the uncertainty in the absolute location of the melting points, both sets of data indicate a larger curvature than the theoretical results. Changing the value of $A_{s,0}$ allows some adjustments of the curvature of the theoretical graphite melting line. Several choices of this strain energy are shown in Fig. 2. Previous work has favored a negative slope for the diamond melting line,[50] which allows a better fit of Bundy's graphite-melting-line data, but recent experimental results indicate that the slope of the diamond melting line should be positive both below 30 GPa (Ref. 51) and above 100 GPa.[52] The model proposed here remains consistent with existing measurements of the diamond-melting-line slope for reasonable values of $A_{s,0}$.

Higher values of $A_{s,0}$ do produce a larger melting-temperature excursion, but do not significantly change the slopes near the lower ($P_{\mathrm{TP}}=11$ MPa) and upper ($P_{\mathrm{TP}}=13$ GPa) triple points. We may note that the largest choice of $A_{s,0}$ causes a positive d^2P/dT_m^2 above 5 GPa, a curvature not generally observed. Figure 2 also shows that stabilizing the fluid diamond phase by an arbitrary 12% decrease of $T_{m,0}$ [Eqs. (13) and (16a)] does not produce a better fit to the experimental data above 70 GPa. It essentially moves the upper triple point to lower temperatures. Accepting the analysis of Ref. 50 and the positive diamond melting line, we must conclude that the experimental data should show a larger pressure increase with decreasing temperature above 70 GPa, consistent with the results of this model.

Given all of the above constraints, the most reasonable shape of the graphite melting line indicates values for $A_{s,0}$ between 2 and 2.4. This implies that the transformation of diamond to graphite is initiated by nucleation sites of five to seven atoms and $\varepsilon^* \approx A_{s,0}kT = 0.8-1.1$ eV, at $T=4500-5500$ K, based on the measured Arrhenius activation energies for the transformation of graphite to diamond[45] mentioned above.

The most significant result of this work is the possible two-phase character of the liquid. The lower value of $A_{s,0}$ gives a uniform fluid phase without transitions, while increasing $A_{s,0}$ results in a liquid-liquid phase separation. Figure 3 is a three-dimensional plot of isotherms in the P,ρ,T plane for the case $A_{s,0}=2.4$. Isotherms between 4000 and 6200 K are shown. The figure contains the graphite-diamond-liquid triple point. Their densities are given in Table. I. Between the graphite-liquid-liquid triple-point and the graphite-liquid-liquid triple-point and the graphite-diamond-liquid triple-point temperatures, the graphite phase separates the low-pressure (graphitic-liquid-rich) and the high-pressure (diamond-like-liquid-rich) liquid phases. The value of $T\,\Delta S$ changes from 1.35 to 0.65 eV between the 0.011 and 13 GPa triple points for $A_{s,0}=2.4$ and varies from 1.31 to 0.65 for $A_{s,0}=2.0$. At the 5.6-GPa triple point, $T\,\Delta S$ is 1.2 or 0.9 eV for transitions to the low- or high-density liquids, respectively. These values bracket the 1.1-eV value measured by Bundy[16] with his millisecond-pulse heating method. The liquid-liquid phase separation has a slope $(dT/dP)_m = 270$ K/GPa, ending in a critical point. The liquidus and graphite solidus terminate in the densities of the graphite-liquid-gas triple point at 11 MPa, nearly 0 on this scale.

TABLE I. Calculated points on the phase diagram of carbon.

Type	T K	P GPa	V cm^3/mol	Phase
			3.588	diamond
Triple point	4570	13.04	4.816	graphite
			3.695	liquid
			5.50	graphite
Triple point	5135	5.61	4.61	liquid
			6.58	liquid
			6.39	graphite
Triple point	~4550	(0.011)	10.80	liquid
			?	vapor
Critical point	5520	7.05	5.17	liquid

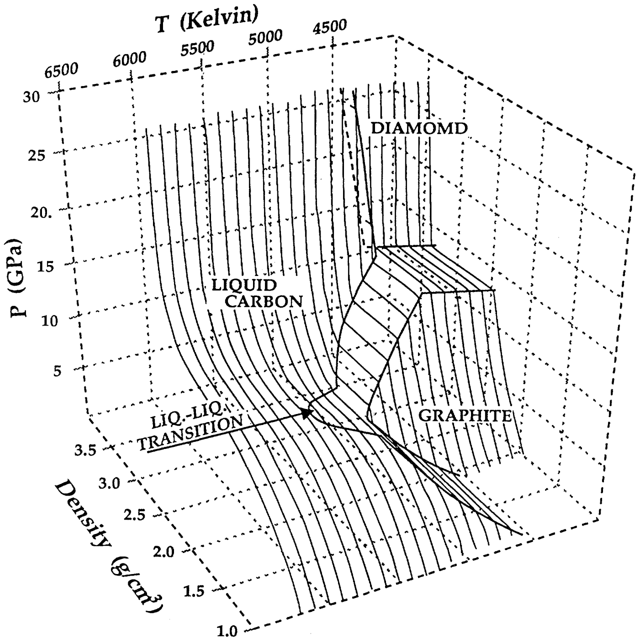

FIG. 3. (P,ρ,T) surface of carbon for $A_{s,0}=2.4$, showing graphite, diamond, and liquid phases as well as the two-phase regions. Isotherms from $T=4000$ to 6200 K are shown.

The liquid-liquid transition affects the shape of the 5000–6000-K isotherms. The corollary of this effect is the extreme compressibility of liquid graphite in this temperature density range. Consistent with this model,

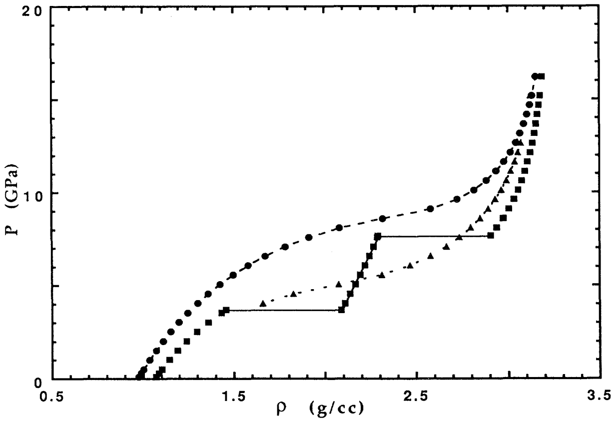

FIG. 4. Liquid-carbon and graphite isotherms: liquid carbon for $A_{s,0}=2.0$ at $T=5000$ K (▲); for $A_{s,0}=2.4$ and $T=5000$ K, a graphite region between 2.1 and 2.3 g/cm^3 and liquid below 1.5 and above 2.9 g/cm^3 (■); and for $A_{s,0}=2.4$ and $T=6000$ K (●).

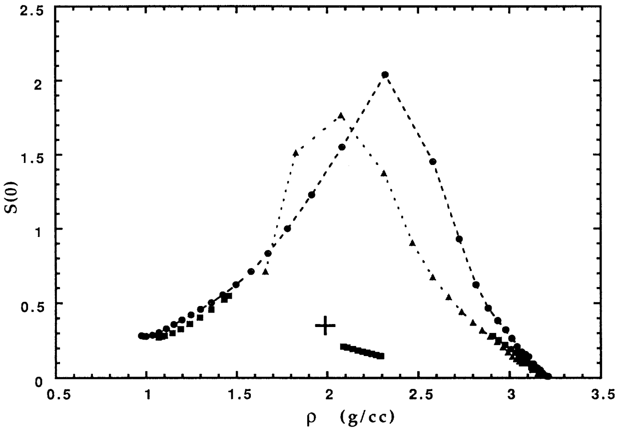

FIG. 5. Structure factors $S(k=0)$ for the isotherms in Fig. 4. Symbols ▲, ■, ● as shown in Fig. 4; (+) result of Dharma-wardana and Perrot (Ref. 53).

density-functional calculations of Dharma-Wardana and Perrot[53] show a significantly large structure factor $S(0)=0.36$ near $\rho=2$ g/cm^3 and $T=5000$ K ($P\sim5$ GPa based on the present model).

Some 5000- and 6000-K isotherms are shown in Fig. 4 for both $A_{s,0}=2.0$ and 2.4. The 5000-K isotherm, for the case $A_{s,0}=2.4$, contains a solid graphite section of intermediate density with lower- and higher-density sections in the liquid phase. The other two isotherms are in the uniform liquid phase and show no volume discontinuities. The volume excursion is large in the transition region between graphitic and diamondlike liquids. Figure 5 details the behavior of $S(0)$. The value of $S(0)=\infty$ in the transition regions between liquid and solid. As a result of these large volume excursions, the values of $S(0)$ calculated here are also large in the diamondlike-to-graphitic transition region of the liquid. The 2-g/cm^3 density, used by Ref. 53, falls in the middle of this region. Their value of $S(0)$ ($=0.36$) is comparatively modest compared to the results of this model and closer to the value for hot graphite. It will be important to explore the above P,ρ,T region with methods such as those of Ref. 13 and 53. Determining the pressures that correspond to the ρ and T selected offers a more accurate comparison with experiment.

VI. SUMMARY

The present work and phase changes observed in other materials indicate the possibility of a liquid-liquid transition in carbon. This possibility needs thorough experimental and theoretical investigation. A review of the available data for liquid graphite indicates general agreement on the conductivity within a factor of 3 (except for liquefied amorphous graphite) and an indication of a possible structural change between the upper and lower triple points because of an increase in conductivity with pressure.

We described the significant aspects of a multiphase carbon model that includes a liquid-mixture model. The solid Grüneisen equations of state for diamond and graphite are fitted to experimental shock-wave and static-compression data with a Birch form for $T=0$ K and a thermodynamically consistent Grüneisen γ_l for nuclear thermal pressures. An electronic Grüneisen term is added to correct for the small electronic thermal pressures and energies at high P and T. Solid nuclear heat capacities are Einstein forms with entropy and energy corrected to give the exact experimental values at standard temperature and pressure. Graphite and diamond-liquid equations of state are obtained with a scaling model, developed by Grover, that is based on a scaled liquid heat capacity and an entropy of melting term that are consistent with experimental heat capacities of low melting metals and melting calculations of soft- and hard-sphere systems. Selected entropies of melting are listed in the text. The model also uses an isotropic Lindemann melting model, which was modified for graphite because of its anisotropy. The c-axis scaling function $[f(V)]$ was selected to maximize the curvature of the graphite melting line.

A liquid-mixing model contains a strain energy A_s. We have shown that Arhenius kinetics and *a priori* quantum-mechanical calculations offer a range of liquid-liquid strain energies, $kTA_{s,0}$ in Eq. (16), between 7 and 0.33 eV. The phase diagram is presented and the experimental data indicate that $kTA_{s,0}\approx1.1$ eV is a reasonable number. With this strain energy, the present model offers good agreement with the experimental shape of the graphite and the diamond melting lines. Such an energy also results in a liquid-liquid phase separation, which terminates in a critical point. The model predicts large compressibilities in the ρ,T range where the graphitic structure of the liquid changes to a diamondlike structure, qualitatively consistent with results from density-functional theory.[53]

ACKNOWLEDGMENTS

This work was performed under the auspices of the U.S. Department of Energy by the Lawrence Livermore National Laboratory under Contract No. 7405-ENG-48.

---

[1] M. van Thiel and F. H. Ree, High Press. Res. **10**, 607 (1992).
[2] K. Tsuji, J. Noncryst. Solids **117/118**, 27 (1990).
[3] S. V. Popova (private communication).
[4] H. Endo, K. Tamura, and M. Yao, Can. J. Phys. **65**, 266 (1987).
[5] V. V. Brazhkin, R. N. Voloshin, and S. V. Popova, in *High Pressure Science and Technology,* edited by W. B. Holzapfel and P. G. Johansen (Gordon and Breach, New York, 1990), p. 348.
[6] V. V. Brazhkin, S. V. Popova, R. N. Voloshin, and A. G. Umnov, High Press. Res. **6**, 363 (1992).
[7] V. V. Brazhkin, R. N. Voloshin, S. V. Popova, and A. G. Umnov, Phys. Lett. A **154**, 413 (1991).
[8] D. A. Young, *Phase Diagrams of the Elements* (University of California Press, Berkeley, 1976), p. 104.
[9] A. Feraz and M. H. Marsh, Phys. Chem. Liq. **8**, 289 (1979). See also A. C. Mitus and A. Z.Patashinskii, Acta Phys. Pol. A

74, 779 (1988).

[10] M. A. Sheindlin, Teplofizika Vysokikh Temperatur **19**, 630 (1981), English translation (Plenum, New York, 1981).

[11] F. P. Bundy, Physica A **156**, 169 (1989).

[12] Per Gustafson, Carbon **24**, 169 (1986).

[13] G. Galli, R. Martin, R. Car, and M. Parrinello, Phys. Rev. B **42**, 7470 (1990); Phys. Rev. Lett. **63**, 988 (1989).

[14] G. Galli, R. Martin, R. Car, and M. Parrinello, Science **250**, 1547 (1990).

[15] Gmelins Handbuch der Anorganischen Chemie-Kohlenstof, part B-issue 2, Syst. No. 14 (Verlag Chemie. GMBH, Weinheim/Bergstrasse, 1968), p. 14.

[16] F. P. Bundy, J. Chem. Phys. **38**, 618 (1963).

[17] D. H. Reitze, H. Ahn, and M. C. Downer, Phys. Rev. B **45**, 2677 (1992).

[18] G. R. Gathers, J. W. Shaner, and D. A. Young (unpublished).

[19] A. V. Baitin, A. A. Lebedev, S. V. Romanenko, V. N. Senchenko, and M. A. Sheindlin, High Temp. High Press. **21**, 157 (1990).

[20] E. Steinbeck, G. Dresselhaus, and M. S. Dresselhaus, Int. J. Thermophys. **11**, 789 (1990); J. Heremans, C. H. Olk, G. L. Esley, J. Steinbeck, and G. Dresselhaus, Phys. Rev. Lett. **60**, 452 (1988).

[21] A. M. Malvezzi, Int. J. Thermophys. **11**, 797 (1990); A. M. Malvezzi, N. Bloembergen, and C. Y. Huang, Phys. Rev. Lett. **57**, 146 (1986).

[22] K. Seibert, D. C. Cho, W. Kütt, H. Kurtz, D. H. Reitze, J. I. Dadap, H. Ahn, M. C. Downer, and A. M. Malvezzi, Phys. Rev. B **42**, 2842 (1990).

[23] J. Heremans and C. P. Beetz, Jr., Phys. Rev. B **32**, 1981 (1985).

[24] A. G. Whittaker, Nature **267**, 695 (1968).

[25] M. van Thiel and F. H. Ree, Int. J. Thermophys. **10**, 227 (1989).

[26] S. Fahey and S. G. Louie, Phys. Rev. B **36**, 6673 (1987).

[27] *Compendium of Shock Wave Data,* edited by M. van Thiel (NTIS, NBS, Springfield, Virginia, 1977), Vol. 1, p. 31ff.

[28] A. K. McMahan, Phys. Rev. B **30**, 5835 (1984).

[29] D. A. Liberman, Phys. Rev. B **20**, 4981 (1979); see also B. I. Bennet and D. A. Liberman (unpublished).

[30] R. Grover, in *Proceedings of the Seventh Symposium on Thermodynamic Properties,* Gaithersburg, MD, 1977, edited by A. Cezairliyan (American Society of Mechanical Engineers, New York, 1977), p. 67.

[31] W. G. Hoover and F. H. Ree, J. Chem. Phys. **49**, 3609 (1968).

[32] W. G. Hoover, S. G. Gray, and K. W. Johnson, J. Chem. Phys. **55**, 1128 (1971).

[33] R. Grover, J. Chem. Phys. **55**, 3435 (1971).

[34] F. A. Lindemann, Z. Phys. **11**, 609 (1910).

[35] E. A. Kraut and G. C. Kennedy, Phys. Rev. **151**, 668 (1966).

[36] R. K. Crawford and W. P. Daniels, Phys. Rev. Lett. **21**, 367 (1968).

[37] V. V. Kechin, High Temp. High Press. **21**, 297 (1989).

[38] M. van Thiel (unpublished).

[39] W. C. Morgan, Carbon **10**, 73 (1972).

[40] S. Fahy, S. G. Louie, and M. Cohen, Phys. Rev. B **34**, 1191 (1986).

[41] E. Rapoport, J. Chem. Phys. **46**, 289 (1967).

[42] P. J. Robinson and K. A. Holbrook, *Unimolecular Reactions* (Wiley-Interscience, New York, 1972).

[43] D. K. C. MacDonald, *Introductory Statistical Mechanics for Physicists* (Wiley, New York, 1963), Appendix II.

[44] F. P. Bundy, J. Chem. Phys. **38**, 631 (1963).

[45] C. Mailhiot and A. K. McMahan, Phys. Rev. B **44**, 11 578 (1991).

[46] S. Hirano, K. Shimono, and S. Naka, J. Mater. Sci. **17**, 1856 (1982).

[47] N. S. Fateeva and L. F. Vereshchagin, Pis'ma Zh. Eksp. Teor. Fiz. **13**, 157 (1971) [JETP Lett. **13**, 110 (1971)].

[48] M. J. Basset, J. Phys. Radium **10**, 217 (1939).

[49] A. Cezairliyan and A. P. Miiller, Int. J. Thermophys. **11**, 643 (1990); (private communication).

[50] I. A. Korunskaya, D. S. Kamenetskaya, and I. L. Aptekar, Fiz. Met. Metalloved. **34**, 942 (1972) [Phys. Met. Metallogr. (USSR) **34**, 39 (1972)].

[51] M. S. Weathers and W. A. Bassett, Phys. Chem. Miner. **15**, 105 (1987).

[52] J. W. Shaner, J. M. Brown, C. A. Swenson, and R. G. McQueen, J. Phys. (Paris) Colloq. **45**, C8-235 (1984).

[53] N. W. C. Dharma-Wardana and Francois Perrot, Phys. Rev. Lett. **65**, 76 (1990).